CHAPTER – 7

MOLECULAR MODELING AND SPECTRAL COMPARISON FOR THE CHANGE IN METHYL POSITION OF NITROPHENOL COMPOUNDS 2-METHYL-4-NITROPHENOL AND 3-METHYL-4-NITROPHENOL: A DENSITY FUNCTIONAL THEORETICAL STUDY

Nitroaromatic compounds are extensively used in the manufacturing of pharmaceuticals, pesticides, plasticizers, azo dyes and explosives [135-137]. Nitrophenolic compounds can accumulate in the soil as a result of hydrolysis of several insecticides such as parathion, methyl parathion, and fenitrothion [137, 138-140] and cause adverse effects to the biological systems. The title compounds 2-methyl-4-nitrophenol and 3-methyl-4-nitrophenol also known as 4-nitro-o-cresol (PNOC) and 4-nitro-m-cresol (PNMC) respectively belong to the group of nitrophenol compounds. These nitrophenol derivatives are used as an intermediate for the synthesis of pesticides. The accumulation of PNMC in the environment from the diesel exhaust particles has serious effects on wildlife and human beings. Through toxic effects on the hypothalamus, pituitary and testis, PNMC disrupts reproductive function in male quail [141]. Environmental oxidative toxicant PNMC caused cytotoxicity in testicular cells of embryonic chicken [142]. In the crystal structure of 2-methyl-4-nitrophenol and 3-methyl-4-nitrophenol, the molecules are linked into a network by the inter-molecular O−H···O and C−H···O interactions which may be effective in the stabilization of the molecular structure [143, 144].

Various spectroscopic studies have been reported on nitrophenol compounds. Complete vibrational assignments of 3-methyl-2-nitrophenol have been reported [145]. Vibrational modes of 2-nitrophenol have been discussed based on SQMFF method [146]. Normal coordinate analysis of p-nitrophenol on the basis of Wilson's GF matrix method has been studied [147].The IR spectrum of 3-methyl-4-nitrophenol

has been analyzed earlier based on the theory proposed by Varsanyi [148]. In this work, detailed vibrational and electronic structure theory studies of 2-methyl-4-nitrophenol and 3-methyl-4-nitrophenol have been performed using the scaled quantum mechanical force field technique based on DFT calculations. Natural bond orbital (NBO) analysis has been done to interpret the charge transfer within the molecule.

7.1 Experimental details

7.1.1 Sample preparation

The compounds PNOC of 97% and PNMC of 98% purity have been purchased from Sigma-Aldrich. Pale yellow crystals of the title compounds were obtained when solid PNOC & PNMC was dissolved in methanol and ethanol respectively, filtered and left for crystallization by slow evaporation of the solvent at room temperature.

7.1.2 IR and Raman measurements

The Fourier-transform infrared spectra of the compounds PNOC and PNMC was recorded in the region 4000 – 400 cm^{-1} using the standard KBr pellet technique with the Jasco FT/IR-6300 instrument. The resolution of the spectrum is 4 cm^{-1}. The Fourier-transform Raman spectrum of PNOC and PNMC was recorded in the region 3500 – 50 cm^{-1} with the resolution of 4 cm^{-1}using FT-Raman Bruker RFS 100/S instrument. An air cooled Nd:YAG laser of 1064nm wavelength and 150mW power is used as the exciting source. The standard Germanium was used as the detector.

7.2 Optimized geometries

The geometrical parameters of PNOC and PNMC calculated by B3LYP/6−31G (d) level is listed in Tables 7.1 and 7.2 are in accordance with the atom numbering scheme of the molecular structure shown in Fig. 7.1.

Table 7.1 Bond lengths and Bond angles of PNOC and PNMC by B3LYP/6-31G (d) in comparison with the XRD data.

2-Methyl-4-nitrophenol (PNOC)						3-Methyl-4-nitrophenol (PNMC)					
Bond length	**Calc. (Å)**	**Expt. [143] (Å)**	**Bond angle**	**Calc. (°)**	**Expt. [143] (°)**	**Bond length**	**Calc. (Å)**	**Expt. [144] (Å)**	**Bond angle**	**Calc. (°)**	**Expt. [144] (°)**
$C_1–C_2$	1.411	1.392	$C_2–C_1–C_6$	121.23	121.53	$C_1–C_2$	1.398	1.390	$C_2–C_1–C_6$	120.04	120.29
$C_1–C_6$	1.401	1.383	$C_2–C_1–O_{10}$	122.11	122.65	$C_1–C_6$	1.400	1.394	$C_2–C_1–O_{10}$	122.49	122.68
$C_1–O_{10}$	1.359	1.357	$C_6–C_1–O_{10}$	116.64	116.82	$C_1–O_{10}$	1.358	1.350	$C_6–C_1–O_{10}$	117.46	117.03
$C_2–C_3$	1.392	1.379	$C_1–C_2–C_3$	118.00	117.66	$C_2–C_3$	1.398	1.393	$C_1–C_2–C_3$	122.39	122.20
$C_2–C_{12}$	1.510	1.496	$C_1–C_2–C_{12}$	120.48	121.27	$C_2–H_9$	1.088	0.929	$C_1–C_2–H_9$	119.10	118.88
$C_3–C_4$	1.394	1.378	$C_3–C_2–C_{12}$	121.51	121.07	$C_3–C_4$	1.412	1.404	$C_3–C_2–H_9$	118.50	118.92
$C_3–H_9$	1.083	0.930	$C_2–C_3–C_4$	120.37	120.44	$C_3–C_{12}$	1.509	1.511	$C_2–C_3–C_4$	116.37	115.82
$C_4–C_5$	1.395	1.382	$C_2–C_3–H_9$	120.69	119.76	$C_4–C_5$	1.401	1.394	$C_2–C_3–C_{12}$	118.04	118.13
$C_4–N_{16}$	1.461	1.451	$C_4–C_3–H_9$	118.93	119.80	$C_4–N_{16}$	1.464	1.450	$C_4–C_3–C_{12}$	125.58	126.03
$C_5–C_6$	1.386	1.370	$C_3–C_4–C_5$	121.52	121.64	$C_5–C_6$	1.382	1.367	$C_3–C_4–C_5$	121.51	122.36
$C_5–H_8$	1.082	0.931	$C_3–C_4–N_{16}$	119.11	119.87	$C_5–H_8$	1.082	0.930	$C_3–C_4–N_{16}$	122.22	121.43
$C_6–H_7$	1.084	0.930	$C_5–C_4–N_{16}$	119.35	118.48	$C_6–H_7$	1.084	0.930	$C_5–C_4–N_{16}$	116.25	116.21
$O_{10}–H_{11}$	0.969	0.820	$C_4–C_5–H_8$	119.64	120.82	$C_{12}–H_{13}$	1.094	0.960	$C_4–C_5–H_8$	118.22	119.83
$C_{12}–H_{13}$	1.099	0.961	$C_6–C_5–H_8$	121.58	120.82	$C_{12}–H_{14}$	1.093	0.960	$C_6–C_5–H_8$	120.89	119.86
$C_{12}–H_{14}$	1.099	0.960	$C_1–C_6–C_5$	120.08	120.33	$C_{12}–H_{15}$	1.093	0.960	$C_1–C_6–C_5$	118.80	119.00
$C_{12}–H_{15}$	1.092	0.960	$C_1–C_6–H_7$	118.64	119.82	$N_{16}–O_{17}$	1.233	1.236	$C_1–C_6–H_7$	119.61	120.48
$N_{16}–O_{17}$	1.232	1.225	$C_5–C_6–H_7$	121.26	119.85	$N_{16}–O_{18}$	1.234	1.215	$C_5–C_6–H_7$	121.58	120.52
$N_{16}–O_{18}$	1.233	1.217	$C_2–C_{12}–H_{13}$	112.05	109.46	-	-	-	$C_3–C_{12}–H_{13}$	109.73	109.48
-	-	-	$H_{13}–C_{12}–H_{14}$	107.64	109.49	-	-	-	$H_{13}–C_{12}–H_{14}$	108.89	109.45
-	-	-	$H_{13}–C_{12}–H_{15}$	107.01	109.41	-	-	-	$H_{13}–C_{12}–H_{15}$	108.89	109.42
-	-	-	$H_{14}–C_{12}–H_{15}$	107.01	109.50	-	-	-	$H_{14}–C_{12}–H_{15}$	106.07	109.51
-	-	-	$C_4–N_{16}–O_{18}$	117.88	118.40	-	-	-	$C_4–N_{16}–O_{18}$	118.66	120.43
-	-	-	$O_{17}–N_{16}–O_{18}$	124.32	122.90	-	-	-	$O_{17}–N_{16}–O_{18}$	123.46	121.28

Table 7.2 Dihedral angles of PNOC and PNMC by B3LYP/6-31G (d) in comparison with the XRD data.

2-Methyl-4-nitrophenol (PNOC)			3-Methyl-4-nitrophenol (PNMC)		
Dihedral angle	**Calc. (°)**	**Expt. [143] (°)**	**Dihedral angle**	**Calc. (°)**	**Expt. [144] (°)**
$C_6–C_1– C_2–C_3$	0.00	1.71	$C_6–C_1– C_2–C_3$	0.00	1.53
$C_6–C_1– C_2–C_{12}$	-179.99	-178.39	$C_6–C_1– C_2–H_9$	180.00	-178.43
$O_{10}–C_1–C_2–C_3$	180.00	178.43	$O_{10}–C_1–C_2–C_3$	179.99	-178.07
$O_{10}–C_1–C_2–C_{12}$	0.00	1.48	$O_{10}–C_1–C_2–H_9$	-0.00	1.97
$C_2–C_1–C_6–C_5$	-0.00	-0.46	$C_2–C_1–C_6–C_5$	-0.00	-0.74
$C_2–C_1–C_6–H_7$	179.99	179.42	$C_2–C_1–C_6–H_7$	-180.00	179.24
$O_{10}–C_1–C_6–C_5$	179.99	179.67	$O_{10}–C_1–C_6–C_5$	180.00	178.88
$O_{10}–C_1–C_6–H_7$	-0.00	-0.45	$O_{10}–C_1–C_6–H_7$	0.00	-1.14
$C_2–C_1–O_{10}–H_{11}$	-0.00	0.66	$C_2–C_1–O_{10}–H_{11}$	0.00	7.14
$C_6–C_1–O_{10}–H_{11}$	179.99	-179.47	$C_6–C_1–O_{10}–H_{11}$	-180.00	-172.48
$C_1–C_2–C_3–C_4$	0.00	-1.48	$C_1–C_2–C_3–C_4$	0.00	-0.96
$C_1–C_2–C_3–H_9$	-179.99	178.49	$C_1–C_2–C_3–C_{12}$	180.00	-179.67
$C_{12}–C_2–C_3–C_4$	-180.00	178.61	$H_9–C_2–C_3–C_4$	-179.99	179.00
$C_{12}–C_2–C_3–H_9$	0.00	-1.42	$H_9–C_2–C_3–C_{12}$	0.00	0.29
$C_1–C_2–C_{12}–H_{13}$	60.58	56.57	$C_2–C_3–C_{12}–H_{13}$	-0.01	8.16
$C_1–C_2–C_{12}–H_{14}$	-60.54	-63.43	$C_2–C_3–C_{12}–H_{14}$	-120.79	-111.82
$C_1–C_2–C_{12}–H_{15}$	-179.97	176.52	$C_2–C_3–C_{12}–H_{15}$	120.75	128.12
$C_3–C_2–C_{12}–H_{13}$	-119.40	-123.52	$C_4–C_3–C_{12}–H_{13}$	179.98	-170.41
$C_3–C_2–C_{12}–H_{14}$	119.45	116.47	$C_4–C_3–C_{12}–H_{14}$	59.20	69.61
$C_3–C_2–C_{12}–H_{15}$	0.02	-3.58	$C_4–C_3–C_{12}–H_{15}$	-59.24	-50.45
$H_9–C_3–C_4–C_5$	179.99	-179.94	$C_{12}–C_3–C_4–C_5$	-180.00	178.24
$H_9–C_3–C_4–N_{16}$	-0.00	-1.23	$C_{12}–C_3–C_4–N_{16}$	-0.00	-1.49
$C_3–C_4–C_5–C_6$	-0.00	1.25	$C_3–C_4–C_5–C_6$	-0.00	1.11
$C_3–C_4–C_5–H_8$	179.99	-178.77	$C_3–C_4–C_5–H_8$	179.99	-178.87
$N_{16}–C_4–C_5–C_6$	180.00	-177.48	$N_{16}–C_4–C_5–C_6$	179.99	-179.15
$N_{16}–C_4–C_5–H_8$	0.00	2.51	$N_{16}–C_4–C_5–H_8$	-0.00	0.88
$C_3–C_4–N_{16}–O_{17}$	180.05	178.64	$C_3–C_4–N_{16}–O_{17}$	-179.95	165.86
$C_3–C_4–N_{16}–O_{18}$	0.04	-1.49	$C_3–C_4–N_{16}–O_{18}$	0.04	-14.53
$C_5–C_4–N_{16}–O_{17}$	0.04	-2.61	$C_5–C_4–N_{16}–O_{17}$	0.04	-13.89
$C_5–C_4–N_{16}–O_{18}$	-179.95	177.26	$C_5–C_4–N_{16}–O_{18}$	-179.95	165.73
$C_4–C_5–C_6–C_1$	0.00	-1.02	$C_4–C_5–C_6–C_1$	0.00	-0.54
$C_4–C_5–C_6–H_7$	-179.99	179.10	$C_4–C_5–C_6–H_7$	-179.99	179.49
$H_8–C_5–C_6–C_1$	-179.99	178.99	$H_8–C_5–C_6–C_1$	-179.99	179.44
$H_8–C_5–C_6–H_7$	0.00	-0.89	$H_8–C_5–C_6–H_7$	0.00	-0.54

The calculated data agrees well with the experimental data [143, 144] except some deviation which is due to the intermolecular interaction in the crystalline state. The C−C bond length in the ring varies from 1.38−1.41Å. This loss of symmetry is due to the various substituents in the phenyl ring. A slight increase in the computed O−H and N−O distances is due to the involvement of these bonds in the inter-molecular interaction in the crystalline state. The $H_9\cdots O_{18}$ and $H_8\cdots O_{17}$ distance is 2.386Å and 2.286Å which is significantly shorter than that of the van der Waals separation between the O atom and the H atom (2.72Å) [98] indicating the existence of C−H...O intra-molecular interaction in PNOC and PNMC respectively.

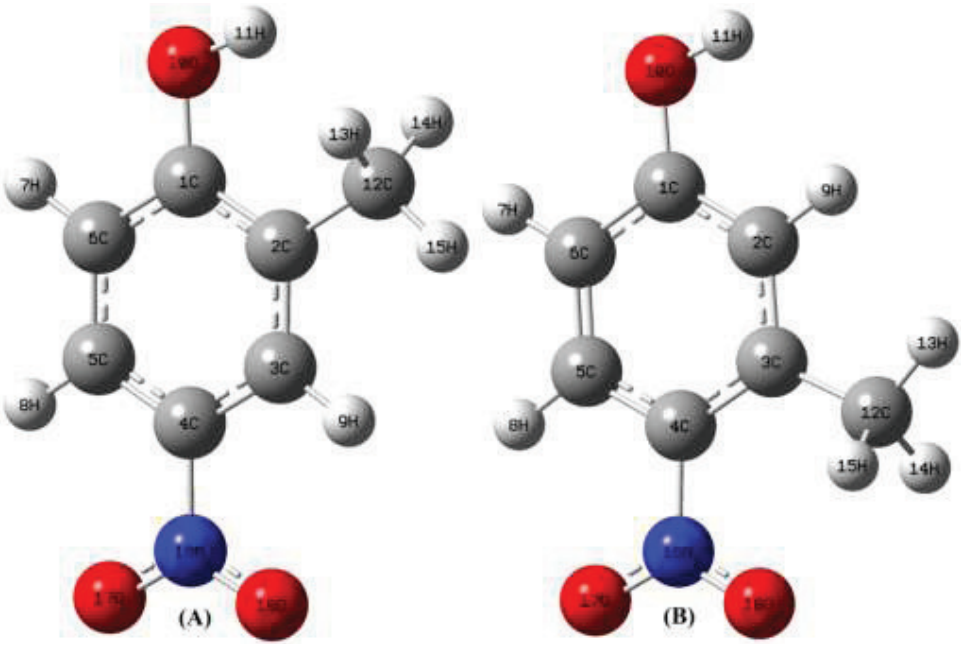

Fig. 7.1 Optimized molecular structure and atomic numbering of (A) PNOC and (B) PNMC.

A decrease in the *endo* angles of $C_1-C_2-C_3$ (118.0° in PNOC) and $C_2-C_3-C_4$ (116.37° in PNMC) and the corresponding increase in the *endo* angles of $C_2-C_1-C_6$,

C_3–C_4–C_5 (121.23°, 121.52° in PNOC) and C_1–C_2–C_3, C_3–C_4–C_5 (122.39°, 121.51° in PNMC) is due to the attachment of electron donating methyl group in the phenyl ring. The variation in *exo* angles C_4–C_3–H_9 and C_2–C_3–H_9 (118.93° and 120.69° respectively in PNOC) bond angles from 120° indicates that C_3–H_9 bonds are slanted towards the NO_2 group forming the intra-molecular hydrogen bond. The *exo* angles C_4–C_5–H_8 and C_6–C_5–H_8 are 118.22° and 120.89° respectively in PNMC are deviated from 120° indicating the slanting of C_5–H_8 bond towards the NO_2 group forming the intra-molecular hydrogen bond. The enlargement of *exo* angle C_4–C_3–C_{12} of 125.58° in PNMC shows the steric repulsion between the methyl and the nitro groups. The global minimum energies for PNOC and PNMC are obtained as -551.2875 a.u and -551.2837 a.u respectively.

7.3 NBO Analysis

NBO analysis provides information about interactions in both filled and virtual orbital spaces that could enhance the analysis of intra- and inter-molecular interactions. Larger the E(2) value, the interaction between electron donors and electron acceptors is more intensive and greater the extent of conjugation of the whole system. Delocalization of electron density between occupied NBO orbitals and unoccupied NBO orbitals correspond to a stabilizing donor-acceptor interaction.

The intra-molecular hyperconjugative interaction (Table 7.3) in PNOC is formed by the orbital overlap between the $\pi(C_1–C_6)$ and $\pi^*(C_2–C_3)$, $\pi^*(C_4–C_5)$ resulting in the stabilization energy of 16.47 and 26.02 kcalmol^{-1} respectively. Another energetic interaction is of $\pi(C_2–C_3)$ with $\pi^*(C_1–C_6)$, $\pi^*(C_4–C_5)$ with energies 23.06 and 17.04 kcalmol^{-1} respectively. The intra-molecular charge transfer from the

phenyl ring to the electron withdrawing nitro group is revealed by the hyperconjugative interaction of $\pi(C_4-C_5)$ with $\pi^*(N_{16}-O_{17})$ with the energy of 27.17 kcalmol^{-1}. The charge transfer from the methyl group to the phenyl ring is revealed by the interaction of the methyl orbitals [$\sigma(C_{12} - H_{13})$ and $\sigma(C_{12} - H_{14})$] with the geminal $\pi^*(C_2-C_3)$ orbitals. The stabilization energy of 29.79 kcalmol^{-1} shows that the lone pair gets donated from the O_{10} atom of the hydroxyl group into the aromatic system. The less energetic contribution of 0.55 kcalmol^{-1} supports the weak intra-molecular $C_3-H_9\ldots O_{18}$ interaction within the molecule.

The intra-molecular hyperconjugative interaction in PNMC is formed by the orbital overlap between the $\pi(C_1-C_2)$ and $\pi^*(C_3-C_4)$, $\pi^*(C_5-C_6)$ resulting in the stabilization energy of 26.00 and 13.89 kcalmol^{-1} respectively. Another energetic interaction is of $\pi(C_3-C_4)$ with $\pi^*(C_1-C_2)$, $\pi^*(C_5-C_6)$ with energies 14.86 and 23.32 kcalmol^{-1} respectively. The hyperconjugative interaction of $\pi(C_3-C_4)$ with $\pi^*(N_{16}-O_{18})$ stabilizes the system with the energy of 29.33 kcalmol^{-1}. The intra-molecular charge transfer from the methyl group to the phenyl ring is revealed by the interaction of the methyl orbitals [$\sigma(C_{12} - H_{14})$ and $\sigma(C_{12} - H_{15})$] with the geminal $\pi^*(C_3-C_4)$ orbitals. The stabilization energy of 31.73 kcalmol^{-1} shows that the lone pair gets donated from the O_{10} atom of the hydroxyl group into the aromatic system. The less energetic contribution of 0.79 kcalmol^{-1} supports the intra-molecular $C_5-H_8\cdots O_{17}$ interaction within the molecule.

Table 7.3 Second order perturbation theory analysis of Fock matrix in NBO basis.

2-Methyl-4-nitrophenol (PNOC)					3-Methyl-4-nitrophenol (PNMC)				
Donor NBO (i)	**ED (i) (e)**	**Acceptor NBO (j)**	**ED (j) (e)**	**E(2) Kcal/mol[a]**	**Donor NBO (i)**	**ED (i) (e)**	**Acceptor NBO (j)**	**ED (j) (e)**	**E(2) Kcal/mol[a]**
$\pi(C_1 - C_6)$	1.606	$\pi^*(C_2 - C_3)$	0.323	16.47	$\pi(C_1 - C_2)$	1.636	$\pi^*(C_3 - C_4)$	0.414	26.00
$\pi(C_1 - C_6)$	1.606	$\pi^*(C_4 - C_5)$	0.408	26.02	$\pi(C_1 - C_2)$	1.636	$\pi^*(C_5 - C_6)$	0.287	13.89
$\pi(C_2 - C_3)$	1.685	$\pi^*(C_1 - C_6)$	0.379	23.06	$\pi(C_3 - C_4)$	1.631	$\pi^*(C_1 - C_2)$	0.388	14.86
$\pi(C_2 - C_3)$	1.685	$\pi^*(C_4 - C_5)$	0.408	17.04	$\pi(C_3 - C_4)$	1.631	$\pi^*(C_5 - C_6)$	0.287	23.32
$\pi(C_4 - C_5)$	1.645	$\pi^*(N_{16} - O_{17})$	0.638	27.17	$\pi(C_3 - C_4)$	1.631	$\pi^*(N_{16} - O_{18})$	0.645	29.33
$\sigma(O_{10} - H_{11})$	1.988	$\sigma^*(C_1 - C_6)$	0.023	4.66	$\sigma(O_{10} - H_{11})$	1.988	$\sigma^*(C_1 - C_6)$	0.025	4.97
$\sigma(C_{12} - H_{13})$	1.982	$\sigma^*(C_2 - C_3)$	0.020	1.80	$\sigma(C_{12} - H_{13})$	1.989	$\sigma^*(C_3 - C_4)$	0.414	4.73
$\sigma(C_{12} - H_{13})$	1.982	$\pi^*(C_2 - C_3)$	0.323	2.78	$\sigma(C_{12} - H_{14})$	1.975	$\sigma^*(C_2 - C_3)$	0.019	1.60
$\sigma(C_{12} - H_{14})$	1.982	$\sigma^*(C_2 - C_3)$	0.020	1.80	$\sigma(C_{12} - H_{14})$	1.975	$\pi^*(C_3 - C_4)$	0.414	3.46
$\sigma(C_{12} - H_{14})$	1.982	$\pi^*(C_2 - C_3)$	0.323	2.77	$\sigma(C_{12} - H_{15})$	1.975	$\sigma^*(C_2 - C_3)$	0.019	1.60
$\sigma(C_{12} - H_{15})$	1.988	$\sigma^*(C_1 - C_2)$	0.035	4.21	$\sigma(C_{12} - H_{15})$	1.975	$\pi^*(C_3 - C_4)$	0.414	3.46
$n_2(O_{10})$	1.851	$\pi^*(C_1 - C_6)$	0.379	29.79	$n_2(O_{10})$	1.853	$\pi^*(C_1 - C_2)$	0.388	31.73
$n_2(O_{18})$	1.899	$\sigma^*(C_3 - H_9)$	0.014	0.55	$n_2(O_{17})$	1.896	$\sigma^*(C_5 - H_8)$	0.014	0.79
$n_2(O_{17})$	1.899	$\sigma^*(C_4 - N_{16})$	0.099	12.17	$n_2(O_{17})$	1.896	$\sigma^*(N_{16} - O_{18})$	0.056	18.95
$n_2(O_{17})$	1.899	$\sigma^*(N_{16} - O_{18})$	0.056	19.23	$n_2(O_{18})$	1.900	$\sigma^*(C_{12} - H_{13})$	0.009	1.34
$n_2(O_{18})$	1.899	$\sigma^*(C_4 - N_{16})$	0.099	12.12	$n_2(O_{18})$	1.900	$\sigma^*(N_{16} - O_{17})$	0.056	19.28

[a] E(2) means energy of hyperconjugative interactions.

7.4 Vibrational Analysis

The vibrational spectral analysis of the compounds 2-methyl-4-nitrophenol and 3-methyl-4-nitrophenol were done based on normal coordinate analysis followed by scaled quantum mechanical force field calculations. The title compounds consist of 18 atoms, and hence 48 normal modes of vibration. Internal valence coordinates of the compounds PNOC and PNMC has been defined in Tables 7.4 and 7.5.

Table 7.4 Definition of internal valence coordinates of 2-methyl-4-nitrophenol.

No.	Symbol	Type	Definition
Stretching			
1-6	R_i	C–C (ring)	C_1–C_2, C_2–C_3, C_3–C_4, C_4–C_5, C_5–C_6, C_6–C_1
7-9	r_i	C–H (ring)	C_3–H_9, C_5–H_8, C_6–H_7
10	η_i	C–O (ring)	C_1–O_{10}
11	P_i	O–H	O_{10}–H_{11}
12	Q_i	C–C (methyl)	C_2–C_{12}
13-15	r_i	C–H (methyl)	C_{12}–H_{13}, C_{12}–H_{14}, C_7–H_{15}
16	η_i	C–N (nitro)	C_4–N_{16}
17-18	ξ_i	N–O (nitro)	N_{16}–O_{17}, N_{16}–O_{18}
Bending			
19-24	β_i	C–C–H (ring)	C_1–C_6–H_7, C_5–C_6–H_7, C_4–C_5–H_8, C_6–C_5–H_8, C_2–C_3–H_9, C_4–C_3–H_9
25-26	β_i	C–C–O (ring)	C_2–C_1–O_{10}, C_6–C_1–O_{10}
27-28	α_i	C–C–C (methyl)	C_1–C_2–C_{12}, C_3–C_2–C_{12}
29-34	δ_i	C–C–C (ring)	C_6–C_1–C_2, C_1–C_2–C_3, C_2–C_3–C_4, C_3–C_4–C_5, C_4–C_5–C_6, C_5–C_6–C_1
35-36	θ_i	C–C–N (nitro)	C_3–C_4–N_{16}, C_5–C_4–N_{16}
37-39	α_i	H–C–H (methyl)	H_{13}–C_{12}–H_{14}, H_{13}–C_{12}–H_{15}, H_{14}–C_{12}–H_{15}
40-42	β_i	C–C–H (methyl)	C_2–C_{12}–H_{13}, C_2–C_{12}–H_{14}, C_2–C_{12}–H_{15}
43-44	β_i	C–N–O (nitro)	C_4–N_{16}–O_{17}, C_4–N_{16}–O_{18}
45	α_i	O–N–O (nitro)	O_{17}–N_{16}–O_{18}

No.	Symbol	Type	Definition
46	Φ_i	C–O–H	C_1–O_{10}–H_{11}
Out-of-plane bending (wagging)			
47-49	ω_i	C–H (ring)	H_7–C_6–C_1–C_5, H_8–C_5–C_6–C_4, H_9–C_3–C_4–C_2.
50	ω_i	C–O (ring)	O_{10}–C_1–C_2–C_6
51	ω_i	C–C (methyl)	C_{12}–C_2–C_1–C_3
52	ω_i	N–O (nitro)	C_4–N_{16}–O_{17}–O_{18}
53	ω_i	C–N (nitro)	N_{16}–C_4–C_5–C_3
Torsion			
54-59	τ_i	*t*CH_3	H_{13}–C_{12}–C_2–C_1, H_{13}–C_{12}–C_2–C_3, H_{14}–C_{12}–C_2–C_1, H_{14}–C_{12}–C_2–C_3, H_{15}–C_{12}–C_2–C_1, H_{15}–C_{12}–C_2–C_3
60-63	τ_i	*t*NO	O_{17}–N_{16}–C_4–C_5, O_{17}–N_{16}–C_4–C_3, O_{18}–N_{16}–C_4–C_5, O_{18}–N_{16}–C_4–C_3
64-65	τ_i	*t*OH	C_2–C_1–O_{10}–H_{11}, C_6–C_1–O_{10}–H_{11}
66-71	τ_i	*t*C-C (ring)	C_6–C_1–C_2–C_3, C_1–C_2–C_3–C_4, C_2–C_3–C_4–C_5, C_3–C_4–C_5–C_6, C_4–C_5–C_6–C_1, C_5–C_6–C_1–C_2

Table 7.5 Definition of internal valence coordinates of 3-methyl-4-nitrophenol.

No.	Symbol	Type	Definition
Stretching			
1-6	R_i	C–C (ring)	C_1–C_2, C_2–C_3, C_3–C_4, C_4–C_5, C_5–C_6, C_6–C_1
7-9	r_i	C–H (ring)	C_2–H_9, C_5–H_8, C_6–H_7
10	η_i	C–O (ring)	C_1–O_{10}
11	P_i	O–H	O_{10}–H_{11}
12	Q_i	C–C (methyl)	C_3–C_{12}
13-15	r_i	C–H (methyl)	C_{12}–H_{13}, C_{12}–H_{14}, C_7–H_{15}
16	η_i	C–N (nitro)	C_4–N_{16}
17-18	ξ_i	N–O (nitro)	N_{16}–O_{17}, N_{16}–O_{18}
Bending			
19-24	β_i	C–C–H (ring)	C_1–C_6–H_7, C_5–C_6–H_7, C_4–C_5–H_8, C_6–C_5–H_8, C_1–C_2–H_9, C_3–C_2–H_9
25-26	β_i	C–C–O (ring)	C_2–C_1–O_{10}, C_6–C_1–O_{10}

No.	Symbol	Type	Definition
27-28	α_i	C–C–C (methyl)	C_2–C_3–C_{12}, C_4–C_3–C_{12}
29-34	δ_i	C–C–C (ring)	C_6–C_1–C_2, C_1–C_2–C_3, C_2–C_3–C_4, C_3–C_4–C_5, C_4–C_5–C_6, C_5–C_6–C_1
35-36	θ_i	C–C–N (nitro)	C_3–C_4–N_{16}, C_5–C_4–N_{16}
37-39	α_i	H–C–H (methyl)	H_{13}–C_{12}–H_{14}, H_{13}–C_{12}–H_{15}, H_{14}–C_{12}–H_{15}
40-42	β_i	C–C–H (methyl)	C_3–C_{12}–H_{13}, C_3–C_{12}–H_{14}, C_3–C_{12}–H_{15}
43-44	β_i	C–N–O (nitro)	C_4–N_{16}–O_{17}, C_4–N_{16}–O_{18}
45	α_i	O–N–O (nitro)	O_{17}–N_{16}–O_{18}
46	Φ_i	C–O–H	C_1–O_{10}–H_{11}
Out-of-plane bending (wagging)			
47-49	ω_i	C–H (ring)	H_7–C_6–C_1–C_5, H_8–C_5–C_6–C_4, H_9–C_2–C_3–C_1.
50	ω_i	C–O (ring)	O_{10}–C_1–C_2–C_6
51	ω_i	C–C (methyl)	C_{12}–C_3–C_4–C_2
52	ω_i	N–O (nitro)	C_4–N_{16}–O_{17}–O_{18}
53	ω_i	C–N (nitro)	N_{16}–C_4–C_5–C_3
Torsion			
54-59	τ_i	*t*CH_3	H_{13}–C_{12}–C_3–C_2, H_{13}–C_{12}–C_3–C_4, H_{14}–C_{12}–C_3–C_2, H_{14}–C_{12}–C_3–C_4, H_{15}–C_{12}–C_3–C_2, H_{15}–C_{12}–C_3–C_4
60-63	τ_i	*t*NO	O_{17}–N_{16}–C_4–C_5, O_{17}–N_{16}–C_4–C_3, O_{18}–N_{16}–C_4–C_5, O_{18}–N_{16}–C_4–C_3
64-65	τ_i	*t*OH	C_2–C_1–O_{10}–H_{11}, C_6–C_1–O_{10}–H_{11}
66-71	τ_i	*t*C-C (ring)	C_6–C_1–C_2–C_3, C_1–C_2–C_3–C_4, C_2–C_3–C_4–C_5, C_3–C_4–C_5–C_6, C_4–C_5–C_6–C_1, C_5–C_6–C_1–C_2,

Force constants of the local symmetry coordinates of PNOC and PNMC and the scale factors used are given in Tables 7.6 and 7.7 respectively. Scale factors have been refined with an RMS error of 4.73 and 5.46 cm^{-1} between the experimental and SQM force field frequencies for PNOC and PNMC respectively. The FT-IR and FT-Raman spectra of both the title compounds were shown in Fig. 7.2 and Fig. 7.3 (3600-

2500 cm^{-1} region), Fig. 7.4 (2500-50 cm^{-1} region) respectively. The vibrational analyses (Table 7.4) of various functional groups are discussed below:

7.4.1 Phenyl ring vibrations

The various normal modes of asymmetric trisubstituted phenyl ring are made according to Wilson's numbering scheme [99]. The bands at 3074, 3050 and 3091, 3047 cm^{-1} in the FT-Raman spectra of PNOC and PNMC respectively are assigned to C-H stretching vibrations. The normal modes 8a, 8b, 19a, 19b and 14 are assigned to C-C stretching vibrations. The modes 8a and 8b for asymmetric trisubstituted benzene ring are observed in the range 1560 – 1610 cm^{-1} and 1571 – 1642 cm^{-1} [99]. The strong intense band at 1587 cm^{-1} in the FT-IR and medium intense band at 1585 cm^{-1} in the FT-Raman spectra is assigned to the 8a mode of PNOC. The 8a mode of PNMC is observed as a strong intense band at 1588 cm^{-1} and medium intense band at 1594 cm^{-1} in the FT-IR and FT-Raman spectra respectively. The mode 8b of PNOC and PNMC is found to be higher than 8a which is observed at 1622 cm^{-1} and 1607 cm^{-1} respectively in the FT-IR spectra. Medium intense band at 1419 cm^{-1} in the FT-IR spectra of PNMC is assigned to mode 19a. The bands at 1458 and 1459 cm^{-1} in the IR spectrum indicate the 19b mode of PNOC and PNMC respectively. The ring mode 14 is observed at 1240 – 1290 cm^{-1} [99] and it is found at 1287 cm^{-1} in IR and its counterpart in Raman at 1286 cm^{-1} for PNOC. Mode 14 is found at 1257 cm^{-1} for PNMC. The allowed C-H in plane bending vibrational modes for asymmetric trisubstituted benzene ring is 3, 15 and 18b. The strong intense band at 1156 cm^{-1} in the IR spectrum of PNOC is assigned to mode 15. Vibrational mode 18b for PNOC is observed as medium intense band at 1090 cm^{-1} in IR and weak band at 1091 cm^{-1} in Raman. Strong band at 1074 cm^{-1} in FT-IR spectrum is assigned to mode 18b of PNMC.

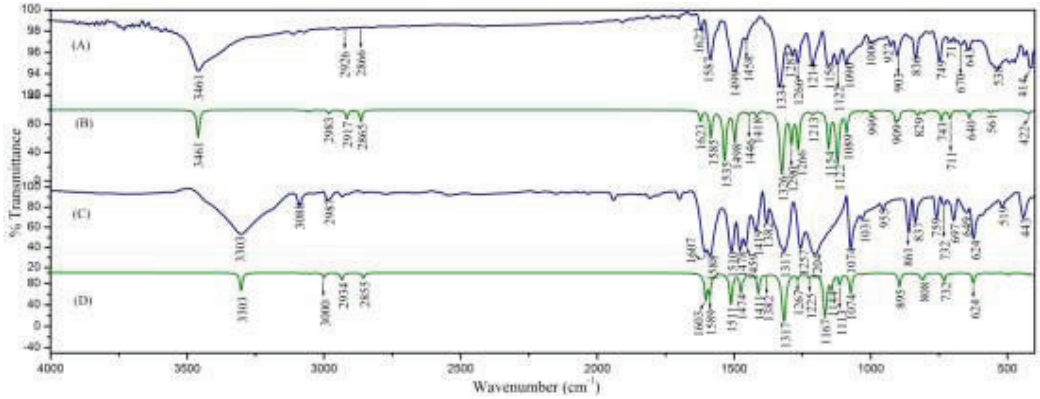

Fig. 7.2 Experimental and simulated IR spectra of PNOC (A, B) and PNMC (C, D) respectively.

Table 7.6 Definition of local symmetry coordinates (much like the natural internal coordinates) of PNOC and the corresponding force constant (mdyne/A_) with scale factors used.

No.	Symbol	Definition	Scale factors	Force constants (mdyne/Å)
Stretching				
1-6	CCs	R_1, R_2, R_3, R_4, R_5, R_6	0.935	6.226
7-9	CHs	r_7, r_8, r_9	0.898	5.120
10	COs	η_{10}	0.873	5.832
11	OHs	P_{11}	0.850	6.709
12	CCme	Q_{12}	0.771	3.618
13	CH_{3ss}	$(r_{13}+r_{14}+r_{15})/\sqrt{3}$	0.902	4.800
14	CH_{3ips}	$(2r_{13}-r_{14}-r_{15})/\sqrt{6}$	0.915	4.698
15	CH_{3ops}	$(r_{14}-r_{15})/\sqrt{2}$	0.890	4.659
16	CNs	η_{16}	0.922	4.203
17	NO_{ss}	$(\xi_{17}+\xi_{18})/\sqrt{2}$	0.927	10.833
18	NO_{ips}	$(\xi_{17}-\xi_{18})/\sqrt{2}$	0.893	8.090
Bending				
19-21	bCH	$(\beta_{19}-\beta_{20})/\sqrt{2}$, $(\beta_{21}-\beta_{22})/\sqrt{2}$, $(\beta_{23}-\beta_{24})/\sqrt{2}$	0.995	0.511
22	bCO	$(\beta_{25}-\beta_{26})/\sqrt{2}$	1.135	1.281

No.	Symbol	Definition	Scale factors	Force constants (mdyne/Å)
23	bCCme	$(\alpha_{27}-\alpha_{28})/\sqrt{2}$	0.751	0.698
24	Rtrid	$(\delta_{29}-\delta_{30}+\delta_{31}-\delta_{32}+\delta_{33}-\delta_{34})/\sqrt{6}$	1.176	1.563
25	Rasyd	$(2\delta_{29}-\delta_{30}-\delta_{31}+2\delta_{32}-\delta_{33}-\delta_{34})/\sqrt{12}$	0.931	1.358
26	Rasydo	$(\delta_{30}-\delta_{31}+\delta_{33}-\delta_{34})/2$	0.982	1.253
27	bCN	$(\theta_{35}-\theta_{36})/\sqrt{2}$	0.951	1.188
28	CH_{3sd}	$(\alpha_{37}+\alpha_{38}+\alpha_{39}-\beta_{40}-\beta_{41}-\beta_{42})/\sqrt{6}$	0.926	0.552
29	CH_{3ipb}	$(2\alpha_{37}-\alpha_{38}-\alpha_{39})/\sqrt{6}$	0.908	0.562
30	CH_{3opb}	$(\alpha_{38}-\alpha_{39})/\sqrt{2}$	0.896	0.562
31	CH_{3ipr}	$(2\beta_{40}-\beta_{41}-\beta_{42})/\sqrt{6}$	0.945	0.644
32	CH_{3opr}	$(\beta_{41}-\beta_{42})/\sqrt{2}$	0.958	0.668
33	NO_{roc}	$(\beta_{43}-\beta_{44})/\sqrt{2}$	0.978	1.378
34	NO_{sci}	$(2\alpha_{45}-\beta_{43}-\beta_{44})/\sqrt{6}$	0.925	1.508
35	bOH	Φ_{46}	0.874	0.739
Out-of-plane bending (wagging)				
36-38	gCH	$\omega_{47}, \omega_{48}, \omega_{49}$	0.938	0.419
39	gOH	ω_{50}	1.157	0.839
40	gCCme	ω_{51}	0.697	0.370
41	gCNO	ω_{52}	0.897	0.502
42	gCN	ω_{53}	0.896	0.469
Torsion				
43	Rpuck	$(\tau_{54}-\tau_{55}+\tau_{56}-\tau_{57}+\tau_{58}-\tau_{59})/\sqrt{6}$	0.905	0.348
44	Rasyt	$(\tau_{54}-\tau_{56}+\tau_{57}-\tau_{59})/2$	1.099	0.351
45	Rasyto	$(-\tau_{54}+2\tau_{55}-\tau_{56}-\tau_{57}+2\tau_{58}-\tau_{59})/\sqrt{12}$	1.067	0.394
46	tCH_3	$(\tau_{60}+\tau_{61}+\tau_{62}+\tau_{63}+\tau_{64}+\tau_{65})/\sqrt{6}$	0.802	0.006
47	tONC	$(\tau_{66}+\tau_{67}+\tau_{68}+\tau_{69})/2$	0.986	0.021
48	tOH	$(\tau_{70}+\tau_{71})/\sqrt{2}$	0.943	0.030

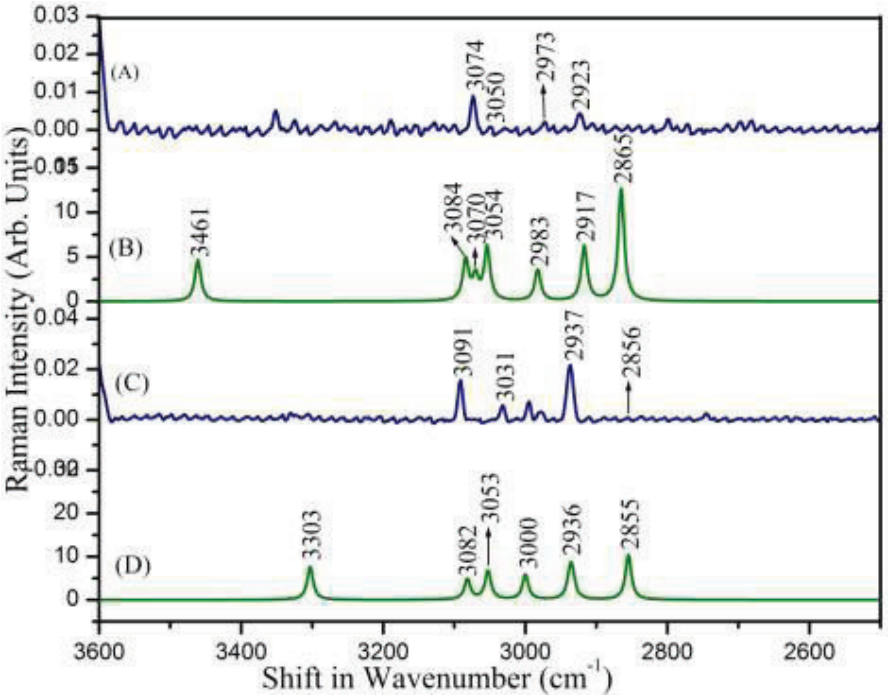

Fig. 7.3 Experimental and simulated Raman spectra of PNOC (A, B) and PNMC (C, D) respectively (3600-2500 cm^{-1} region).

Table 7.7 Definition of local symmetry coordinates (much like the natural internal coordinates) of PNMC and the corresponding force constant (mdyne/A) with scale factors used.

No.	Symbol	Definition	Scale factors	Force constants (mdyne/Å)
Stretching				
1-6	CCs	R_1, R_2, R_3, R_4, R_5, R_6	0.933	6.408
7-9	CHs	r_7, r_8, r_9	0.895	4.947
10	COs	η_{10}	0.705	4.765
11	OHs	P_{11}	0.779	6.109
12	CCme	Q_{12}	0.581	2.730
13	CH_{3ss}	$(r_{13}+r_{14}+r_{15})/\sqrt{3}$	0.867	4.722
14	CH_{3ips}	$(2r_{13}-r_{14}-r_{15})/\sqrt{6}$	0.874	4.643
15	CH_{3ops}	$(r_{14}-r_{15})/\sqrt{2}$	0.875	4.668
16	CNs	η_{16}	0.948	4.225
17	NO_{ss}	$(\xi_{17}+\xi_{18})/\sqrt{2}$	0.903	10.497
18	NO_{ips}	$(\xi_{17}-\xi_{18})/\sqrt{2}$	0.858	7.694

No.	Symbol	Definition	Scale factors	Force constants (mdyne/Å)
Bending				
19-21	bCH	$(\beta_{19}-\beta_{20})/\sqrt{2}$, $(\beta_{21}-\beta_{22})/\sqrt{2}$, $(\beta_{23}-\beta_{24})/\sqrt{2}$	0.950	0.490
22	bCO	$(\beta_{25}-\beta_{26})/\sqrt{2}$	0.852	0.875
23	bCCme	$(\alpha_{27}-\alpha_{28})/\sqrt{2}$	0.581	0.762
24	Rtrid	$(\delta_{29}-\delta_{30}+\delta_{31}-\delta_{32}+\delta_{33}-\delta_{34})/\sqrt{6}$	1.062	1.404
25	Rasyd	$(2\delta_{29}-\delta_{30}-\delta_{31}+2\delta_{32}-\delta_{33}-\delta_{34})/\sqrt{12}$	1.062	1.579
26	Rasydo	$(\delta_{30}-\delta_{31}+\delta_{33}-\delta_{34})/2$	1.062	1.397
27	bCN	$(\theta_{35}-\theta_{36})/\sqrt{2}$	0.948	1.745
28	CH_{3sd}	$(\alpha_{37}+\alpha_{38}+\alpha_{39}-\beta_{40}-\beta_{41}-\beta_{42})/\sqrt{6}$	0.936	0.576
29	CH_{3ipb}	$(2\alpha_{37}-\alpha_{38}-\alpha_{39})/\sqrt{6}$	0.943	0.546
30	CH_{3opb}	$(\alpha_{38}-\alpha_{39})/\sqrt{2}$	1.013	0.603
31	CH_{3ipr}	$(2\beta_{40}-\beta_{41}-\beta_{42})/\sqrt{6}$	0.964	0.751
32	CH_{3opr}	$(\beta_{41}-\beta_{42})/\sqrt{2}$	0.953	0.626
33	NO_{roc}	$(\beta_{43}-\beta_{44})/\sqrt{2}$	1.016	1.498
34	NO_{sci}	$(2\alpha_{45}-\beta_{43}-\beta_{44})/\sqrt{6}$	1.016	1.698
35	bOH	Φ_{46}	1.015	0.854
Out-of-plane bending (wagging)				
36-38	gCH	ω_{47}, ω_{48}, ω_{49}	0.950	0.382
39	gOH	ω_{50}	0.661	0.465
40	gCCme	ω_{51}	0.581	0.343
41	gCNO	ω_{52}	0.935	0.541
42	gCN	ω_{53}	0.981	0.531
Torsion				
43	Rpuck	$(\tau_{54}-\tau_{55}+\tau_{56}-\tau_{57}+\tau_{58}-\tau_{59})/\sqrt{6}$	1.062	0.386
44	Rasyt	$(\tau_{54}-\tau_{56}+\tau_{57}-\tau_{59})/2$	1.062	0.316
45	Rasyto	$(-\tau_{54}+2\tau_{55}-\tau_{56}-\tau_{57}+2\tau_{58}-\tau_{59})/\sqrt{12}$	1.062	0.374
46	tCH_3	$(\tau_{60}+\tau_{61}+\tau_{62}+\tau_{63}+\tau_{64}+\tau_{65})/\sqrt{6}$	0.809	0.016
47	tONC	$(\tau_{66}+\tau_{67}+\tau_{68}+\tau_{69})/\sqrt{4}$	1.195	0.012
48	tOH	$(\tau_{70}+\tau_{71})/\sqrt{2}$	0.880	0.035

7.4.2 Methyl group vibrations

The title compounds PNOC and PNMC possess one methyl group in the second and third position respectively with respect to the hydroxy group in the phenyl

ring. The asymmetric and symmetric stretching vibrations of methyl groups attached to the phenyl ring are usually downshifted due to electronic effects [101] and are expected near 2925 cm^{-1} and 2865 cm^{-1} respectively. The bands at 2926 and 2866 cm^{-1} in FT-IR are assigned to asymmetric and symmetric stretching vibrations respectively of PNOC. For PNMC the asymmetric and symmetric stretching vibrations are obtained at 2934 and 2855 cm^{-1} respectively in the FT-IR. Methyl asymmetric and symmetric deformation vibrations of the methyl substituted benzene derivatives normally appear in the region 1440 − 1465 cm^{-1} and 1370 − 1390 cm^{-1} respectively [102, 103]. Methyl asymmetric deformation mode of PNOC and PNMC is obtained at 1458 and 1478 cm^{-1} respectively in the FT-IR spectra. Bands at 1380 and 1382 cm^{-1} in the FT-IR spectra indicate the methyl symmetric deformation of PNOC and PNMC respectively.

7.4.3 Nitro group vibrations

The asymmetric and symmetric NO_2 stretching vibration of aromatic compounds gives a band in the range 1570 − 1485 cm^{-1} and 1370 − 1320 cm^{-1} [103] respectively. For PNOC very weak band at 1535 cm^{-1} in FT-Raman is assigned to asymmetric stretching vibration. Very strong intense band at 1326 cm^{-1} in FT-Raman spectrum is assigned as symmetric NO_2 stretching vibration of PNOC. The band at 1510 cm^{-1} in the IR is assigned to asymmetric NO_2 stretching vibration of PNMC. The Raman counterpart is obtained at 1515 cm^{-1} with weak intensity. Very strong intense band at 1317 cm^{-1} in FT-Raman spectrum is assigned as symmetric NO_2 stretching vibration of PNMC. The scissoring vibration gives a band in the region 890−835 cm^{-1} [101]. The medium intense band at 837 cm^{-1} in FT-IR is the NO_2 scissoring mode of PNMC.

Table 7.8 Vibrational assignment of PNOC and PNMC by normal coordinate analysis based on SQM force field calculations.

2-Methyl-4-nitrophenol						3-Methyl-4-nitrophenol					
Calculated (DFT)			Observed (cm^{-1})		Assignment (% PED, internal coordinates having contribution ≥10% are shown)	Calculated (DFT)			Observed (cm^{-1})		Assignment (% PED, internal coordinates having contribution ≥10% are shown)
ν_{Scaled} (cm^{-1})	IR intensities (%)	Raman intensities (%)	FT-IR	FT-Raman		ν_{Scaled} (cm^{-1})	IR intensities (%)	Raman intensities (%)	FT-IR	FT-Raman	
3461	21.84	4.69	3461	-	νOH(100)	3303	17.26	7.61	3303	-	νOH(100)
3084	0.42	4.60	-	-	νCH(99)	3082	0.59	4.68	3089	3091	νCH(99)
3070	0.29	2.54	-	3074	νCH(99)	3053	0.63	6.59	3045	3047	νCH(99)
3054	0.92	6.00	-	3050	νCH(99)	3000	4.29	5.73	-	-	νCH(99)
2983	2.40	3.52	-	2973	CH_{3ips}(48) + CH_{3ops}(40) + CH_{3ss}(12)	2937	1.35	4.89	-	2937	CH_{3ops}(100)
2917	5.91	6.19	2926	-	CH_{3ips}(52) + CH_{3ops}(42)	2934	5.21	4.44	2934	-	CH_{3ips}(97)
2865	7.91	12.80	2866	-	CH_{3ss}(82) + CH_{3ops}(17)	2855	4.48	10.25	2855	-	CH_{3ss}(97)
1623	7.10	4.45	1622	-	Ph[νCC(62)] + Ph[δCH(10)]	1603	28.95	9.22	1607	-	Ph[νCC(63)] + Ph[δCH(11)]
1585	21.59	21.63	1587	1585	Ph[νCC(63)] + Ph[δCH(17)]	1589	21.07	12.38	1588	1594	Ph[νCC(61)] + Ph[δCH(14)]
1535	54.75	2.72	-	1535	NO_{2ips}(73)	1512	1.60	5.67	-	-	CH_{3opb}(94)
1498	26.19	0.08	1499	-	Ph[δCH(46)] + Ph[νCC(34)]	1511	36.17	1.71	1510	1515	NO_{2ips}(52) + Ph[νCC(11)]

2-Methyl-4-nitrophenol						3-Methyl-4-nitrophenol					
Calculated (DFT)			Observed (cm^{-1})		Assignment (% PED, internal coordinates having contribution ≥10% are shown)	Calculated (DFT)			Observed (cm^{-1})		Assignment (% PED, internal coordinates having contribution ≥10% are shown)
ν_{Scaled} (cm^{-1})	IR intensities (%)	Raman intensities (%)	FT-IR	FT-Raman		ν_{Scaled} (cm^{-1})	IR intensities (%)	Raman intensities (%)	FT-IR	FT-Raman	
1463	0.49	2.53	1458	-	CH_{3opb}(28) + CH_{3ipb}(26) + Ph[νCC(19)]	1474	19.10	3.37	1478	1475	CH_{3ipb}(50) + NO_{2ips}(13) + CH_{3ipr}(12)
1446	2.44	5.96	-	1448	CH_{3ipb}(60) + CH_{3opb}(29)	1463	1.88	0.34	1459	-	Ph[νCC(34)] + Ph[δCH(27)] + CH_{3ipb}(16) + NO_{2ips}(13)
1418	4.02	2.74	-	1421	Ph[νCC(34)] + CH_{3opb}(28)	1411	20.50	0.98	1419	1423	Ph[δCH(36)] + Ph[νCC(26)] + δOH(16)
1380	1.20	6.84	1380	-	CH_{3sd}(86)	1382	1.32	7.23	1382	1380	CH_{3sd}(87)
1332	4.69	2.14	-	-	Ph[νCC(59)] + Ph[δCH(18)] + δOH(12)	1318	100.00	100.00	1317	1317	NO_{2ss}(54) + νCN(17) + NO_{2sci}(16)
1326	100.00	100.00	1334	1326	NO_{2ss}(60) + νCN(16) + NO_{2sci}(14)	1304	1.40	1.23	-	-	Ph[νCC(69)] + Ph[δCH(11)]
1290	26.25	8.73	1287	1286	Ph[νCC(38)] + Ph[δCH(34)]	1267	4.70	0.47	1257	1257	Ph[δCH(33)] + Ph[νCC(31)]
1266	34.46	8.95	1266	-	νCO(38) + Ph[δCH(21)] + Ph[νCC(19)] + Ph_{trid}(14)	1225	3.82	3.12	1204	1207	Ph[νCC(38)] + Ph[δCH(26)] + δOH(12) + νCO(10)
1213	2.43	9.33	1214	-	Ph_{trid}(32) +	1167	76.07	7.51	-	1174	Ph_{trid}(24) + νCO(23) +

2-Methyl-4-nitrophenol						3-Methyl-4-nitrophenol					
Calculated (DFT)			Observed (cm^{-1})		Assignment (% PED, internal coordinates having contribution ≥10% are shown)	Calculated (DFT)			Observed (cm^{-1})		Assignment (% PED, internal coordinates having contribution ≥10% are shown)
ν_{Scaled} (cm^{-1})	IR intensities (%)	Raman intensities (%)	FT-IR	FT-Raman		ν_{Scaled} (cm^{-1})	IR intensities (%)	Raman intensities (%)	FT-IR	FT-Raman	
					Ph[νCC(21)] + Me[νCC(19)] + δOH(14)						δOH(19)+ Ph[νCC(18)]
1154	34.18	7.66	1156	1159	Ph[δCH(60)] + Ph[νCC(23)]	1144	13.83	9.14	-	1155	Ph[δCH(40)] + Ph[νCC(31)]
1122	61.10	14.61	1122	1126	δOH(42) + Ph[νCC(28)]	1113	9.68	14.56	-	-	Ph[νCC(39)] + Ph[δCH(28)] + νCN(15)
1089	15.82	7.60	1090	1091	Ph[νCC(41)] + Ph[δCH(28)] + νCN(15)	1074	20.37	10.72	1074	1078	Ph_{trid}(28) + Ph[νCC(19)] + CH_{3ipr}(14) + Ph[δCH(12)] + νCN(10)
1033	0.68	0.51	-	1033	CH_{3ipr}(56) + CH_{3opr}(23)	1032	0.94	0.41	1032	-	CH_{3opr}(81)
999	2.84	2.40	1000	-	CH_{3opr}(45) + CH_{3ipr}(19) + Ph[νCC(18)]	1014	0.33	1.49	-	1014	CH_{3ipr}(54) + Ph[νCC(22)]
935	0.24	0.88	-	935	Ph[gCH(90)]	956	0.12	0.67	956	958	Ph[gCH(86)]
909	7.61	5.10	903	-	Me[νCC(21)] + νCN(17) + Ph[νCC(15)] + Ph_{asyd}(15)	895	13.10	16.87	-	-	Ph[νCC(23)] + Me[νCC(18)] + Ph_{asyd}(17) + νCO(15)
899	5.65	0.61	-	893	Ph[gCH(78)]	836	0.79	2.58	837	842	NO_{2sci}(53)

2-Methyl-4-nitrophenol						3-Methyl-4-nitrophenol					
Calculated (DFT)			Observed (cm^{-1})		Assignment (% PED, internal coordinates having contribution ≥10% are shown)	Calculated (DFT)			Observed (cm^{-1})		Assignment (% PED, internal coordinates having contribution ≥10% are shown)
ν_{Scaled} (cm^{-1})	IR intensities (%)	Raman intensities (%)	FT-IR	FT-Raman		ν_{Scaled} (cm^{-1})	IR intensities (%)	Raman intensities (%)	FT-IR	FT-Raman	
828	3.62	2.88	836	-	Ph[gCH(72)] + gOH(13)	817	2.87	2.83	-	-	Ph[gCH(78)]
806	2.31	0.47	-	806	NO_{2sci}(49) + Ph_{trid}(12) + νCO(11)	808	5.40	1.91	-	-	Ph[gCH(83)]
743	7.10	16.31	749	-	Ph[νCC(35)] + Me[νCC(24)] + Ph_{asydo}(16) + νCO(11)	732	7.26	1.75	732	736	NO_2[gNO(50)] + NO_2[gCN(16)] + Ph_{puck}(16) + Ph[gCH(14)]
711	5.76	2.12	711	-	NO_2[gNO(65)] + NO_2[gCN(15)] + Ph_{puck}(11)	710	0.86	7.61	697	-	Ph_{asydo}(50) + Me[νCC(19)] + Ph[νCC(13)]
672	0.85	0.30	670	-	gOH(37) + Ph_{puck}(37) + Ph[gCH(14)]	650	0.07	0.22	649	-	Ph_{puck}(72)
640	5.54	2.79	643	-	Ph_{asydo}(30) + Ph_{asyd}(22) + NO_{2sci}(16) + νCN(11)	624	9.31	0.26	625	626	Ph_{asyd}(28) + νCN(17) + νCO(16) + NO_{2sci}(14) + Ph[νCC(11)]
562	1.80	6.64	-	569	δCO(36) + δCN(15) + NO_{2roc}(14)	554	0.43	10.40	-	-	NO_{2roc}(34) + δCN(26) + Ph[νCC(13)] + Me[νCC(10)]

2-Methyl-4-nitrophenol						3-Methyl-4-nitrophenol					
Calculated (DFT)			Observed (cm^{-1})		Assignment (% PED, internal coordinates having contribution ≥10% are shown)	Calculated (DFT)			Observed (cm^{-1})		Assignment (% PED, internal coordinates having contribution ≥10% are shown)
ν_{Scaled} (cm^{-1})	IR intensities (%)	Raman intensities (%)	FT-IR	FT-Raman		ν_{Scaled} (cm^{-1})	IR intensities (%)	Raman intensities (%)	FT-IR	FT-Raman	
537	0.42	2.13	538	-	NO_{2roc}(41) + Ph_{asydo}(21)	496	1.67	6.60	520	524	Me[νCC(28)] + Ph_{asydo}(24) + NO_{2roc}(17) + Ph[νCC(10)]
519	0.01	0.08	-	520	Ph_{puck}(49) + NO_2[gCN(21)] + Ph_{asyt}(15) + Ph[gCH(12)]	472	0.04	0.09	-	-	Ph_{asyt}(37) + gOH(27) + NO_2[gCN(14)] + Me[gCC(11)]
433	1.20	0.12	-	434	Ph_{asyto}(62) + Me[gCC(17)]	428	1.10	0.08	443	449	Ph_{asyto}(59) + Me[gCC(10)]
422	2.43	8.24	414	-	δCO(30) + NO_{2roc}(21) + Ph_{asydo}(19) + Ph[νCC(10)]	395	1.86	2.38	-	376	δCO(52) + NO_{2roc}(15) + Me[δCC(11)]
354	34.63	4.85	-	354	τOH(91)	383	33.97	7.15	-	-	τOH(87)
353	0.01	5.04	-	-	Ph_{asyd}(48) + νCN(30) + Ph[νCC(10)]	356	0.28	5.12	-	354	Ph_{asyd}(38) + νCN(31)
299	0.01	5.63	-	302	Ph_{puck}(35) + Me[gCC(26)] + Ph_{asyt}(11) + NO_2[gCN(10)]	298	0.19	5.28	-	-	NO_2[gCN(41)] + gOH(25)
285	0.16	1.49	-	285	Me[δCC(59)] +	276	0.45	1.84		306	Me[δCC(84)]

2-Methyl-4-nitrophenol						3-Methyl-4-nitrophenol					
Calculated (DFT)			Observed (cm^{-1})		Assignment (% PED, internal coordinates having contribution ≥10% are shown)	Calculated (DFT)			Observed (cm^{-1})		Assignment (% PED, internal coordinates having contribution ≥10% are shown)
ν_{Scaled} (cm^{-1})	IR intensities (%)	Raman intensities (%)	FT-IR	FT-Raman		ν_{Scaled} (cm^{-1})	IR intensities (%)	Raman intensities (%)	FT-IR	FT-Raman	
					δCO(15) + δCN(10)						
201	0.63	1.96	-	-	δCN(56) + Me[δCC(24)]	237	0.54	4.50	-	-	δCN(46) + Me[δCC(28)] + δCO(11)
177	0.11	21.63	-	138	Me[gCC(53)] + NO_2[gCN(12)] + Ph_{asyt}(11)	222	0.11	4.59	-	221	τCH_3(83)
140	0.54	0.76	-	121	τCH_3(78)	172	0.00	12.38	-	-	Me[gCC(59)] + gOH(15)
110	0.14	6.90	-	86	Ph_{asyt}(29) + NO_2[gCN(19)] + τCH_3(15) + Me[gCC(14)] + Ph_{puck}(13)	106	0.18	21.00	-	-	Ph_{asyt}(54) + NO_2[gCN(19)] + Ph[gCH(10)]
64	0.02	5.42	-	-	τNO_2(88)	18	0.02	65.41	-	-	τNO_2(46) +τCH_3(42)]

Ph, phenyl ring; Me, Methyl; ν, stretching; δ, bending; τ, torsion; g, gauche; ss, symmetric stretching; ips, in plane stretching; ops, out of plane stretching; ipb, in plane bending; opb, out of plane bending; ipr, in plane rocking; opr, out of plane rocking; puck, puckering; trid, trigonal deformation; asyd, asymmetric deformation; asydo, out of plane asymmetric deformation; asyt, asymmetric torsion; asyto, out of plane asymmetric torsion; sci, scissoring.

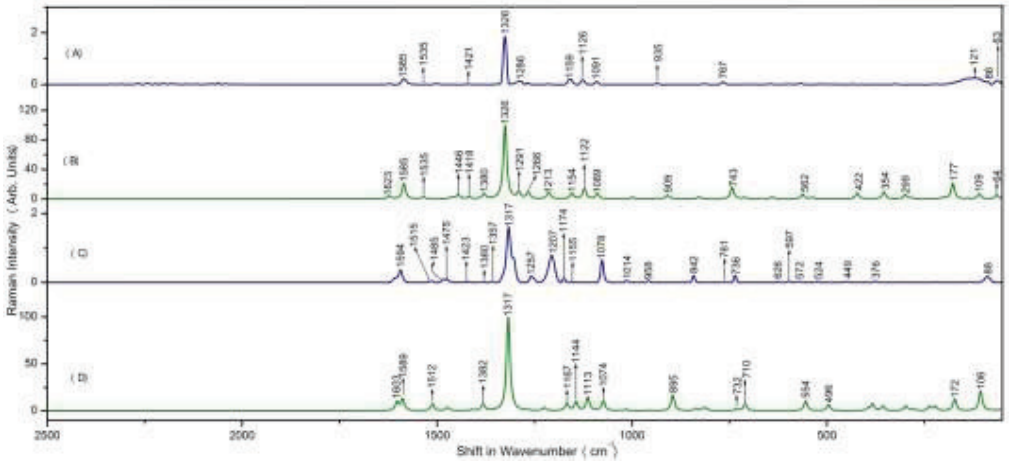

Fig. 7.4 Experimental and simulated Raman spectra of PNOC (A, B) and PNMC (C, D) respectively (2500-50 cm^{-1} region).

7.4.4 Hydroxyl group vibrations

The vibrations corresponding to the hydroxyl group are the stretching and bending vibrations of the CO and OH moieties. The OH stretching of a free molecule appears as a sharp band above 3600 cm^{-1} [30]. The red shifted broad bands at 3461 and 3303 cm^{-1} in the FT-IR spectra corresponds to the OH stretching vibrations of PNOC and PNMC. Sharp bands at 3461 and 3303 cm^{-1} in the theoretical spectra indicate the absence of inter-molecular interaction. PNOC and PNMC are similar compounds with same functional groups, but there is a frequency shift of 158 cm^{-1} in the OH stretching of PNMC when compared to PNOC. This indicates the strong O−H···O interaction of the OH bond of PNMC when compared with PNOC. The medium intense band at 1266 cm^{-1} in FT-IR spectrum is assigned to C−O stretching of PNOC. This vibrational mode appears at 1174 cm^{-1} in FT-Raman spectrum of PNMC. The bands at 1214 and 1204 cm^{-1} in the FT-IR spectra of PNOC and PNMC shows the OH bending vibrational mode.

7.5 Physiochemical properties

A high melting point is due to the strong intermolecular force between the molecules in the compound. The melting point range of PNOC is 93 – 98°C [149] and that of PNMC is 125 − 130°C [150]. Comparing the melting points of PNOC and PNMC there is a variation of 32°C. This indicates that the compound PNMC has strong intermolecular interaction when compared to PNOC. This is also evident from comparing the broadening of OH region in IR spectra of both the compounds. As the position of the methyl group is changed from second to third position the stability of the compound is increased.

7.6 Conclusion

Molecular structure of 2-methyl-4-nitrophenol and 3-methyl-4-nitrohenol were modeled using density functional theoretical method and it agrees well with the experimental structure. A complete vibrational assignment of the two compounds was done using the scaled quantum mechanical force field method. The simulated spectra are plotted and the spectra of both the compounds have been compared. Natural bond orbital analysis confirms the intra-molecular C−H···O interaction. PNOC and PNMC, nitrophenol derivatives with same functional groups and different methyl position show difference in the OH stretching frequency region. The large shift (158 cm^{-1}) in the OH stretching frequency specifies the strength of hydrogen bonding in the crystalline state. The stability of the compound increased as the position of the methyl group is changed from second to third position.